

Ferromagnetism induced by planar nanoscale CuO inclusions in Cu-doped ZnO thin films

C. Sudakar,^{1,*} J. S. Thakur,² G. Lawes,¹ R. Naik,¹ and V. M. Naik³

¹*Department of Physics and Astronomy, Wayne State University, Detroit, Michigan 48201, USA*

²*Department of Electrical and Computer Engineering, Wayne State University, Detroit, Michigan 48202, USA*

³*Department of Natural Sciences, University of Michigan-Dearborn, Dearborn, Michigan 48128, USA*

(Received 13 September 2006; revised manuscript received 17 December 2006; published 28 February 2007)

We report ferromagnetism above 300 K in ZnO: x Cu (x in at. %) sputtered thin films. For $x < 1$, a large magnetic moment of $1.6 \mu_B/\text{Cu}$ was observed, which decreases monotonically with increasing x . We find evidence that the ferromagnetic moment is due to Cu-O planar nanophase inclusions in ZnO basal planes. The presence of CuO nanophase is confirmed by transmission electron microscopy, x-ray diffraction, and Raman spectroscopy studies. These inclusions are present even for $x < 3$, where Cu-O structures of a few nanometers in size are observed. Field-cooled and zero-field-cooled magnetization measurements show a bifurcation for temperatures below 300 K.

DOI: [10.1103/PhysRevB.75.054423](https://doi.org/10.1103/PhysRevB.75.054423)

PACS number(s): 75.50.Pp, 75.70.-i, 75.75.+a, 81.15.Cd

I. INTRODUCTION

For the last two decades, diluted magnetic semiconductors (DMSs) have been extensively studied for potential applications to spintronics and with the goal of identifying doped semiconducting materials with large magnetic moments M and with a high Curie temperature T_C .^{1,2} High values of T_C and M are desired for the operational stability and integrity of spintronic based devices at room temperature. Many DMSs exhibit a T_C well above room temperature and, in particular, ZnO has been identified as a promising host semiconductor material, exhibiting ferromagnetism when doped with most of the transition metal elements—V, Cr, Fe, Co, and Ni.^{3,4} ZnO is also a candidate material for short-wavelength magneto-optical applications because of its large band gap value (3.4 eV).

Among the transition elements, the ferromagnetic behavior of Cu-doped ZnO is not well understood, with conflicting reports on the magnetic properties of this system.⁵⁻¹² Early investigations of its ferromagnetic properties were performed using numerical simulations. Sato and Katayama-Yoshida used *ab initio* calculations and predicted that ZnO:Cu cannot develop ferromagnetic order,⁵ which was later confirmed experimentally.⁶ Using local spin-density approximation, Coulomb correlation, and spin-orbit calculations,⁷ it was shown that for a particular concentration of Cu, i.e., Zn_{0.9375}Cu_{0.0625}O, ZnO:Cu becomes half-metallic, where Cu 3d states are partially occupied atomiclike t_2 states near the Fermi energy E_F and Cu ion is in a 2+ state. This ferromagnetic (FM) phase has a predicted magnetic moment of $\sim 1.0 \mu_B/\text{Cu}$. A different mechanism⁸ involving a distortion in the ZnO lattice on doping with Cu was suggested to induce ferromagnetic coupling between the Cu moments in ZnO:Cu. Recently, using full-potential linearized augmented plane-wave and DMOL³ calculations, it was shown⁹ that ZnO:Cu can develop FM order with a magnetic moment of $\sim 1.0 \mu_B/\text{Cu}$. At a higher concentration of Cu (12.5%), they also observed a competing antiferromagnetic (AFM) phase; however, the FM phase still remained stable by 43 meV against the AFM phase. Using *ab initio* electronic structure calculations, a fundamental insight about the magnetic be-

havior of dopant d bands and its exchange splitting between the occupied and unoccupied 3d states can be obtained. However, the conclusions from these calculations, including the nature of the FM phase, the value of T_C , and other properties, critically depend on the electronic correlations⁵⁻⁷ employed in the calculations. In real systems, disorder arising due to doping introduces additional interaction effects, which can significantly alter magnetic properties and the mechanism for the phase transition.¹³

Experimentally, observations of ferromagnetism in ZnO: x Cu remain unclear. A strong magnetic circular dichroism signal near the band gap of ZnO films was observed¹⁰ when doped with Cu. This indicates the presence of an exchange interaction between sp -band carriers and the d electrons localized on Cu ions and suggests the possibility of realizing ferromagnetic order in Cu-doped ZnO. So far, only very few experiments have observed FM order in ZnO:Cu films and their results are inconclusive.^{8,10-12} One of the problems is that it is difficult to fabricate high-quality samples with controlled dopant concentrations because of the poor solubility of Cu in ZnO due to the strong localization of the Cu 3d states without hybridizing with Zn 4s conduction band. Ferromagnetic hysteresis loops did appear in powder samples, but Cu-doped ZnO films were nonmagnetic.⁸ ZnO:Cu films grown by radio-frequency magnetron sputtering on n -GaN/Al₂O₃ substrate claimed FM order mediated by electrons.¹¹ However, very recently, electron mediated FM order was ruled out in Cu-doped ZnO films grown by pulsed-laser ablation,¹² but p -type films exhibited FM order with $T_C \sim 390$ K, magnetic moment $\sim 0.4 \mu_B/\text{Cu}$, and a coercive field ~ 40 Oe.

Despite a large number of theoretical predictions and experimental investigations, there is still no consensus on the origins of the FM state in ZnO:Cu films. Therefore, it is important to clarify the nature of the ferromagnetism, whether intrinsic or extrinsic, for such a technologically important material. In magnetic thin-film materials, substrate and structural features have been found to strongly influence the magnetic properties. In this paper, we report a systematic investigation of the structural and magnetic properties of ZnO: x Cu films (x in at. %) grown on quartz and sapphire substrates by reactive magnetron cosputtering. Our experi-

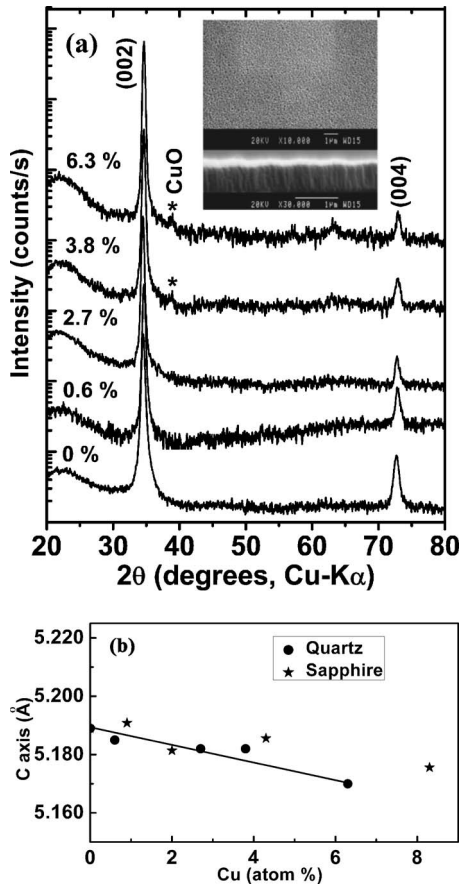


FIG. 1. (a) X-ray diffraction patterns of ZnO: x Cu films on quartz substrate with $x=0.6, 2.7, 3.8,$ and 6.3 at. %. Numbers in the figures denote x . Inset: The topographic and cross-sectional SEM of a typical Cu-doped ZnO. (b) Change in lattice constant c of ZnO: x Cu films (grown on quartz and sapphire substrates) as a function of Cu concentration. The line is a guide to the eyes.

mental observations lead us to conclude that FM in ZnO: x Cu films may originate from planar Cu-O nanophase lying in the basal planes of ZnO crystal.

II. EXPERIMENT

ZnO: x Cu films were deposited by reactive magnetron cosputtering of highly pure (99.99%) metallic zinc and copper targets ($\phi=75$ mm) by using dc and rf power sources. High-purity oxygen and argon were used as the reactive and sputtering gases. The partial pressures of these gases are controlled for precision by using mass flow controllers. The base pressure in the turbo-molecular pumped sputtering chamber was 10^{-6} mbar and the total pressure during deposition was maintained at 1×10^{-3} mbar. The oxygen partial pressure required to deposit zinc oxide films has been optimized to 2×10^{-4} mbar. The rates of deposition from the zinc and copper targets were varied independently by controlling the target power, with a copper target in an off-axis configuration to tune the doping concentration of copper. The typical deposition rate was 4 nm/min, and the films used in the present study had thickness in the range of 500–700 nm. Deposi-

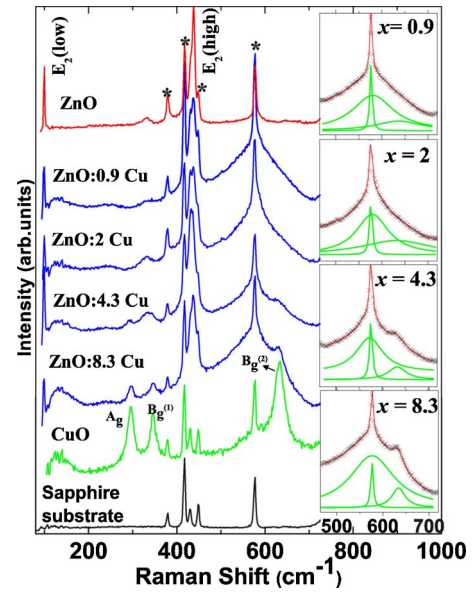


FIG. 2. (Color online) The Raman spectra of Cu-doped ZnO ($x=0-8.3\%$) thin films on sapphire substrate along with CuO film and the bare sapphire substrate. Peaks from the sapphire substrate are indicated by * (cf. the spectra given for pure sapphire substrate). The inset shows the deconvoluted curves. The overlapping sapphire peak is also seen.

tions have been carried out separately on quartz and sapphire (0001) substrates maintained at ambient temperature without any deliberate heating. The substrates were cleaned successively in 10% HCl, distilled water, acetone, and trichloroethylene using ultrasonic agitation, and finally, dry nitrogen fluxing. The films were annealed after deposition *ex situ* in ambient environment at 500°C and characterized by various techniques.

The structural quality of the films was investigated by x-ray diffraction (XRD) using Cu $K\alpha$ radiation, high-resolution transmission electron microscopy (HRTEM), and micro-Raman spectroscopy. Raman spectra were recorded using 514.5 nm excitation line in backscattering geometry [$z(x+y, x+y)\bar{z}$]. In this backscattering geometry with incident light parallel to the c axis, only $E_2, A_1(\text{TO}),$ and $E_1(\text{TO})$ are allowed for wurtzite ZnO. Magnetic measurements were done using a Quantum Design MPMS2 superconducting quantum interference device magnetometer with magnetic field parallel to the film surface.

III. RESULTS

All the ZnO and ZnO: x Cu films are transparent with a smooth surface consisting of uniformly distributed round particles of 30–50 nm. The cross-sectional scanning electron microscope (SEM) micrograph revealed densely packed columnar grains growing perpendicular to the substrate surface [Fig. 1(a), inset]. The average atomic concentration of copper in ZnO films is determined to be in the range of 0–8 at. % using energy dispersive x-ray spectroscopy (EDXS) analysis. The x-ray diffraction patterns of all the films [Fig. 1(a)] show only (00 l) reflections of ZnO. No

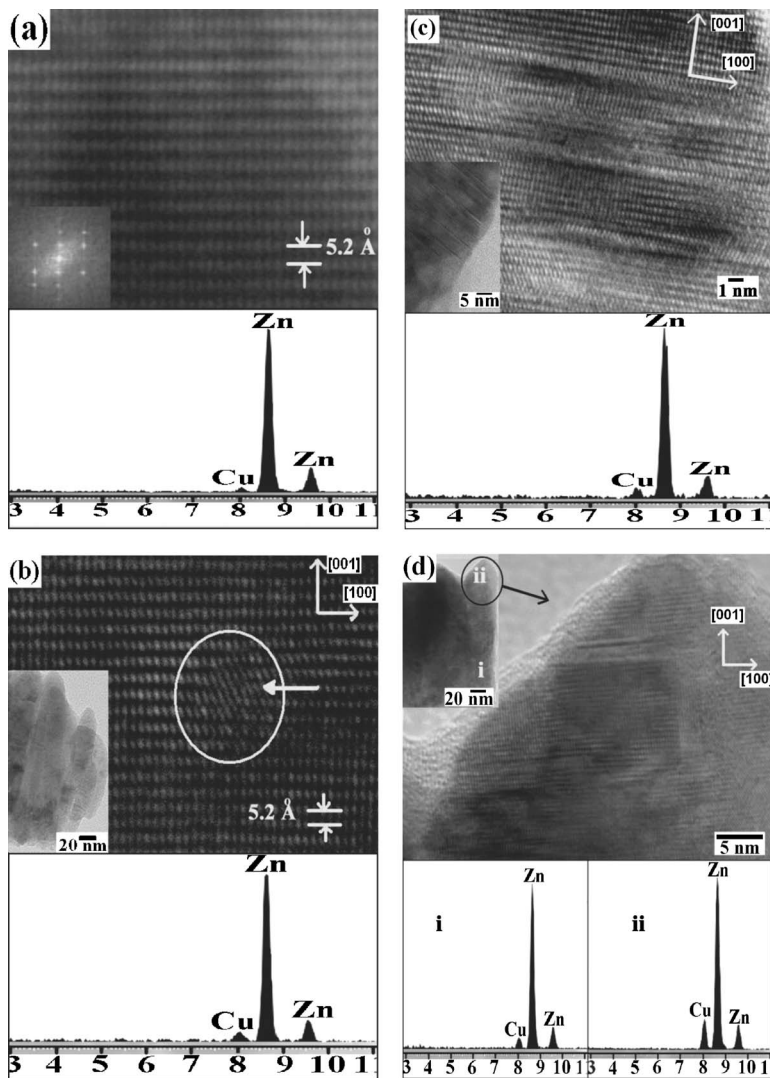


FIG. 3. HRTEM of ZnO: x Cu films with (a) $x=0.6$, (b) $x=2.7$, (c) $x=3.8$, and (d) $x=6.3$ at.%. Inset: (a) Fast Fourier transform of the image along [010] and [(b)–(d)] low magnification images of columnar grains. Formation of a dislocation is shown by an arrow in (b). The bottom panels in each figure show the EDXS spectra from the samples. The x axis shows the x-ray energy (keV). The EDXS spectra shown in the bottom panel of (d) are acquired from the regions marked (i) and (ii) in the inset.

peaks corresponding to copper/copper oxide or any other secondary phases were discerned in the XRD scans for samples with $x < 3$. This indicates that, within the x-ray detection limits, the films are monophasic. In contrast, at higher copper concentration ($x > 3$ at. %), a small CuO peak is detected irrespective of the substrate used. This is associated with the decreased intensity of (00 l) reflections compared to pure ZnO and the appearance of (103) reflection at $2\theta \sim 63^\circ$, which imply some local structural disorder due to Cu doping. The change in the hexagonal lattice constant c of ZnO: x Cu films as a function of Cu concentration is shown in Fig. 1(b). The lattice constant c shows a small decrease with an approximate linear dependence at low Cu concentration but deviates at higher concentrations. The shift in the XRD peak position clearly suggests incorporation of Cu into ZnO lattice without altering the crystal structure.

To investigate the presence of nanoscale sized local structures in these films, we have used micro-Raman spectroscopy. Figure 2 shows the Raman spectra of ZnO, ZnO: x Cu, and CuO sputtered films along with sapphire substrate. At low concentrations ($x < 1\%$) of Cu, the Raman spectrum shows a broad asymmetric mode at ~ 580 cm^{-1} . This mode is attributed to the $E_1(\text{LO})$ mode of ZnO. Although this mode

is not allowed in the scattering geometry used, its observation shows breakdown in the Raman selection rules due to the incorporation of Cu into the ZnO crystal lattice. The broadening of the $E_1(\text{LO})$ mode is due to defects associated with the oxygen sublattice or cation interstitials.¹⁴ At higher concentrations ($>3\%$), this band evolves into two distinct peaks: broad peaks at 580 and 634 cm^{-1} . We have deconvoluted the spectral profiles in the 450–700 cm^{-1} range using a multiple Lorentzian peak fitting procedure. For low concentration samples, a single Lorentzian peak did not fit the peak profile satisfactorily. However, the inclusion of an additional broad peak corresponding to CuO in the fitting process gave a satisfactory fit. Thus the broad asymmetric band ~ 600 cm^{-1} at low concentrations ($<3\%$) was deconvoluted into two distinct peaks ~ 580 and ~ 634 cm^{-1} , which are attributed to $E_1(\text{LO})$ of ZnO and B_g mode of CuO.¹⁵ Distortions in the oxygen sublattice result when CuO nanophase is incorporated into the (001) cationic planes of ZnO at Zn atom positions, with the oxygen atom situated in the adjacent anion planes.¹⁶ The presence of uniformly distributed small nanoscale amounts of Cu-O at concentrations less than 2 at. % does not seem to induce observable distortions in the structure of ZnO as determined from HRTEM.¹⁶ However,

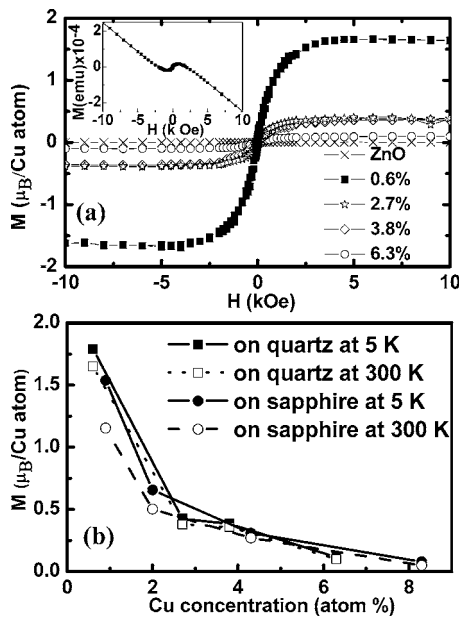


FIG. 4. (a) M - H loops at 300 K for $\text{ZnO}:x\text{Cu}$ (x in at. %) films. Pure ZnO showed diamagnetic behavior. (b) Cu concentration dependent magnetization changes measured at 5 and 300 K. The lines are guides to the eyes. Inset: M - H curve for $\text{ZnO}:0.6\text{Cu}$ before substrate correction.

Raman spectra show evidence for the presence of CuO nanophase in ZnO even at such small dopant concentrations. At 8.3 at. % of Cu very strong bands are observed at 296, 345, and 634 cm^{-1} , which coincide with the Raman spectrum of CuO.¹⁷ It should be noted that the Cu ions remain predominantly in a +2 (d^9) valence state under the present reactive sputter deposition and annealing conditions, as confirmed by x-ray photoelectron spectroscopy.

In order to investigate the dopant distribution, defect structure, or phase segregation correlations for different Cu concentrations, combined HRTEM imaging and EDXS analyses using a focused electron probe has been carried out at a number of locations throughout the specimens. For higher values of x , a nonuniform intensity distribution indicative of numerous defects, likely to be dislocations, is observed. The arrangement of copper in ZnO as planar CuO clusters and the associated dislocations studied by HRTEM are reported by Klenov *et al.*¹⁶ Planar clusters can be incorporated in (001) cationic planes of ZnO at the Zn atom positions, with oxygen atoms situated in the adjacent anion planes. This gives rise to the appearance of a dislocation loop. The atomic weights of CuO and ZnO are not sufficiently different to explain the nonuniform intensity distribution. However, the associated oxygen lattice distortion provides additional contrast in the HRTEM images, as observed in Fig. 3. HRTEM images were taken at different regions on the film and the representative lattice images with Cu-rich regions are shown in Fig. 3. The corresponding EDX spectra are also shown at the bottom panels of each figure. For $\text{ZnO}:x\text{Cu}$ (with $x=0.6$ at. %), the grain interior and grain boundary regions show an ordered structure with no discernible segregation, secondary phases, or clustering of copper cations [Fig. 3(a)]. This is indicative of a homogeneous dis-

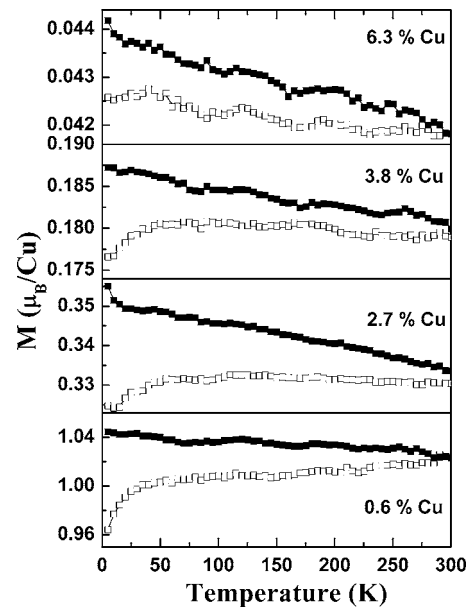


FIG. 5. The magnetization measured at $H=500$ Oe as a function of temperature for $\text{ZnO}:x\text{Cu}$ films. Both zero-field-cooled (open) and field-cooled (filled) curves are shown.

tribution of copper atoms in the ZnO crystal lattice by incorporation into Zn sites or by the presence of small Zn-rich CuO nanophase as interstitials in ZnO.¹⁶ Occasional dislocations seen can be attributed to CuO nanophase segregation within ZnO lattice for $x=2.7$ at. % [Fig. 3(b)]. At higher concentration of Cu ($x=3.8$ and 6.3 at. %), the lattice images exhibit distortions along (001) planes, as seen by the bending/wrinkling of the lattice fringes caused by stacking faults in the atomic rows [Figs. 3(c) and 3(d)]. HRTEM images of such grains with Cu-rich regions clearly suggest that the location of copper atoms within the bulk of the zinc oxide crystals are located along the c planes. In the bottom panel of Fig. 3(d), two regions with different Cu concentrations, corresponding to regions (i) and (ii) marked in the inset, are shown. Thus Cu atoms alloyed with ZnO exist as planar nanophases of Cu-O ($\sim 1-10$ nm) interspersed into the (001) cationic planes of ZnO.

One of the goals of this investigation is to correlate the magnetic properties of $\text{ZnO}:x\text{Cu}$ films with their structural characteristics. Figure 4(a) shows the M - H loops for $\text{ZnO}:x\text{Cu}$ ($x=0.6, 2.7, 3.8,$ and 6.3 at. %) films measured at 300 K with applied field parallel to the film surface, after proper correction for the diamagnetic term arising from the substrate. The inset in Fig. 4(a) shows the M - H loop for $\text{ZnO}:0.6\text{Cu}$ before background correction for the substrate. These hysteresis curves provide evidence for ferromagnetic ordering at room temperature, with a coercive field (H_c) of approximately 50 Oe. The large value of the magnetic moment, M ($\mu_B/\text{Cu atom}$), at 300 K indicates that T_C is well above room temperature, and the moment remains almost constant down to 5 K. We do not observe any significant anisotropy in the magnetization when measured with field perpendicular to the film surface. The dependence of M on Cu concentration in $\text{ZnO}:x\text{Cu}$ films was investigated over a range of x (0–8.3 at. %) values shown in Fig. 4(b) at 5 and

300 K for films grown on different substrates. No significant effects on M due to different substrates were observed. Because we expect the crystallinity and defect concentration of the sample to depend strongly on the choice of substrate, this suggests that the ferromagnetism is relatively insensitive to film quality. Films with $x < 1$ at. % showed a very large value of $M = 1.6 \pm 0.2 \mu_B/\text{Cu}$ at 300 K, and for $x > 1$, M decreases rapidly to $0.4 \pm 0.05 \mu_B/\text{Cu}$ at $x \cong 2$ at. % and $0.1 \mu_B/\text{Cu}$ for $x \cong 6$ at. %. For $x > 2$ at. %, the linear decrease of M with x is similar to that observed by Buchholz *et al.*¹² in their p -type ZnO:Cu films. A large $M \sim 1.85 \mu_B/\text{Cu}$ is predicted for half-metallic Cu-doped ZnO films due to the orbital magnetic-moment contribution to the total moment value of the occupied minority spin t_2 states near the Fermi energy.⁷

These measurements (Raman spectra for different x values, XRD, and HRTEM) suggest that magnetic properties arise from the presence of a Zn-rich CuO nanophase. This is consistent with our observation that the ferromagnetic moment is insensitive to film quality. One of the important signatures of nanosized magnetic particles is the separation of $M(T)$ zero-field-cooled (ZFC) and field-cooled (FC) curves below the blocking temperature, T_B . The magnetic moment is plotted as a function of temperature in Fig. 5 while warming under an applied field of 500 Oe parallel to the film plane for both ZFC and FC protocols. These curves show no magnetic anomaly at the Néel temperature for bulk CuO, which is consistent with previous studies on CuO nanoparticles.¹⁸ The splitting between the FC and ZFC curves strongly suggests the presence of superparamagnetic blocking in magnetic nanoparticles, although it is impossible to definitively rule out some other origin for the bifurcation. Because the maximum temperature for all magnetic measurements was 300 K, we can only state that the proposed superparamagnetic blocking temperature in Cu:ZnO nanoclusters is above 300 K for all samples. The estimated effective magnetic anisotropic constant for these CuO nanophase structures, assuming square clusters with sides ~ 5 nm, considering $T_B = 300$ K (which is expected to underestimate the correct T_B , hence also the value of anisotropy), is $\sim 10^7$ erg/cm³, which is comparable to highly anisotropic magnetic materials.¹⁹

IV. DISCUSSION AND CONCLUSION

In general, two main theoretical models—Ruderman-Kittel-Kasuya-Yosida-type indirect exchange interactions and interactions between bound-magnetic polarons (BMPs)—are used to explain the ferromagnetic order in DMS materials.²⁰ The highly resistive nature and weak correlation between the d orbitals of Cu ions observed⁹ in these films indicate that d - d double exchange is not energetically favorable and would not promote a ferromagnetic transition. In contrast to TiO₂ based FM materials, oxygen vacancies are known to destroy⁹ the FM order in ZnO: x Cu films. Percolation based FM order arising from the formation of BMP does not explain these data. Similarly, the BMP model of Coey *et al.*⁴ can also not induce FM order in these highly resistive films.

The presence of Cu-O planar nanophase may give rise to the ferromagnetism in ZnO:Cu. In the bulk form, CuO crystallizes in the monoclinic space group $C2/c$.²¹ The structure consists of stacks of CuO ladders along $[110]$ and $[\bar{1}10]$ which intersect in the direction of $[001]$ by sharing O²⁻ ions. Experiments show an incommensurate antiferromagnetic phase transition between $T_{N1} = 230$ K and $T_{N2} = 213$ K, with a commensurate AFM phase below T_{N2} .²¹ Small CuO particles are known to acquire ferromagnetic order,²² and the magnetic susceptibility of these CuO nanoparticles increases rapidly when their size decreases. This strong magnetic behavior in nonmagnetic CuO has been attributed to the uncompensated spins of the surface Cu ions in nanoparticles.²² Further, the lattice distortion, as evidenced in the Raman spectra and HRTEM, can promote FM superexchange interaction in Cu-O-Cu complex lying in the basal plane. When cluster sizes are small, e.g., at small Cu doping, the residual spins of the Cu ions at the cluster interface can couple ferromagnetically with planar spins to generate larger values of the moment. The surface field becomes pronounced for small cluster sizes and leads to a dramatic increase in the M values. As the Cu doping increases, the bulklike Cu-O-Cu antiferromagnetic superexchange interaction begins to dominate,^{23,24} which leads to smaller values of M at higher concentration of Cu. We have been unable to identify other extrinsic sources for the observed ferromagnetism, and these films are found to be free from spurious impurities. Furthermore, measurements on pure ZnO films prepared under identical conditions failed to detect any ferromagnetism, ruling out the deposition chamber as a possible source of contamination. Although Cu metal has no spontaneous magnetization, Cu ions can be spin polarized in some compounds, such as the CuO₂ planes in the high-temperature superconductors. Therefore, additional investigations using theoretical calculations on Cu-O planar nanostructures embedded in a ZnO lattice may provide additional insight into the role of these planar structures in producing FM order in nonmagnetic materials.

In conclusion, we argue that ferromagnetism in Cu-doped ZnO originates from the formation of planar CuO nanophase. HRTEM, XRD, and Raman spectral analysis show that Cu ions in ZnO lattice are not uniformly incorporated but form CuO planar nanophase structures in ZnO: x Cu films. ZFC and FC magnetization curves are bifurcated up to 300 K, consistent with the supposition that the magnetic order arises from Zn-rich CuO nanoclusters. The role of these clusters in the development of ferromagnetic order remains to be clarified, but the presence of the nanoscopic secondary phase cannot be neglected for ZnO: x Cu, and should be considered for other transition-metal-doped semiconducting oxides.

ACKNOWLEDGMENTS

J.S.T. is thankful to the support from the Center for Smart Sensors and Integrated Microsystems at Wayne State University, Detroit.

*Author to whom correspondence should be addressed. Electronic address: csudakar@gmail.com

- ¹R. Janisch, P. Gopal, and N. A. Spaldin, *J. Phys.: Condens. Matter* **17**, R657 (2005).
- ²T. Dietl, H. Ohno, F. Matsukura, J. Cibert, and D. Ferrand, *Science* **287**, 1019 (2000).
- ³T. Fukumura, Y. Yamada, H. Toyosaki, T. Hasegawa, H. Koinuma, and M. Kawasaki, *Appl. Surf. Sci.* **223**, 62 (2004).
- ⁴J. M. D. Coey, M. Venkatesan, and C. B. Fitzgerald, *Nat. Mater.* **4**, 173 (2005).
- ⁵K. Sato and H. Katayama-Yoshida, *Jpn. J. Appl. Phys., Part 2* **39**, L555 (2000).
- ⁶Z. Jin, M. Murakami, T. Fukumura, Y. Matsumoto, A. Ohtomo, M. Kawasaki, and H. Koinuma, *J. Cryst. Growth* **214/215**, 55 (2000).
- ⁷M. S. Park and B. I. Min, *Phys. Rev. B* **68**, 224436 (2003).
- ⁸H.-J. Lee, B.-S. Kim, C. R. Cho, and S.-Y. Jeong, *Phys. Status Solidi B* **241**, 1533 (2004).
- ⁹L. H. Ye, A. J. Freeman, and B. Delley, *Phys. Rev. B* **73**, 033203 (2006).
- ¹⁰K. Ando, H. Saito, Z. Jin, T. Fukumura, M. Kawasaki, Y. Motsumoto, and H. Koinuma, *J. Appl. Phys.* **89**, 7284 (2001).
- ¹¹C.-R. Cho, J.-Y. Hwang, J.-P. Kim, S.-Y. Jeong, M.-S. Jang, W.-J. Lee, and D.-H. Kim, *Jpn. J. Appl. Phys., Part 2* **43**, L1383 (2004).
- ¹²D. B. Buchholz, R. P. H. Chang, J. H. Song, and J. B. Ketterson, *Appl. Phys. Lett.* **87**, 082504 (2005).
- ¹³M. Berciu and R. N. Bhatt, *Phys. Rev. Lett.* **87**, 107203 (2001).
- ¹⁴J. N. Zeng, J. K. Low, Z. M. Ren, T. Liew, and Y. F. Lu, *Appl. Surf. Sci.* **197**, 362 (2002).
- ¹⁵G. Kliche and Z. V. Popovic, *Phys. Rev. B* **42**, 10060 (1990).
- ¹⁶D. O. Klenov, G. N. Kryukova, and L. M. Plyasova, *J. Mater. Chem.* **8**, 1665 (1998).
- ¹⁷T. Yu, X. Zhao, Z. X. Shen, Y. H. Wu, and W. H. Su, *J. Cryst. Growth* **268**, 590 (2004).
- ¹⁸X. G. Zheng, T. Mori, K. Nishiyama, W. Higemoto, and C. N. Xu, *Solid State Commun.* **132**, 493 (2004).
- ¹⁹S. Sun, C. B. Murray, D. Weller, L. Folks, and A. Moser, *Science* **287**, 1989 (2000).
- ²⁰T. Dietl, H. Ohno, and F. Matsukura, *Phys. Rev. B* **63**, 195205 (2001).
- ²¹H. Yamada, X. G. Zheng, Y. Soejima, and M. Kawaminami, *Phys. Rev. B* **69**, 104104 (2004).
- ²²A. Punnoose, H. Magnone, M. S. Seehra, and J. Bonevich, *Phys. Rev. B* **64**, 174420 (2001).
- ²³A. Filippetti and V. Fiorentini, *Phys. Rev. Lett.* **95**, 086405 (2005).
- ²⁴X. Feng, *J. Phys.: Condens. Matter* **16**, 4251 (2004).